ADVANCED MATERIALS
www.advmat.de

Fabrication of High-Performance Flexible Alkaline Batteries by Implementing Multiwalled Carbon Nanotubes and Copolymer Separator

*Zhiqian Wang, Zheqiong Wu, Natalia Bramnik, and Somenath Mitra**

In this paper we present the development of a flexible primary alkaline battery with multiwalled carbon nanotube (MWCNT) enhanced composite electrodes and polyvinyl alcohol (PVA)-poly (acrylic acid) (PAA) copolymer separator. MWCNTs were found to be more effective as a conductive additive than graphite. Though more dispersible, carboxylated MWCNTs appeared to increase the resistance of the electrode and decrease the electrochemical performance, whereas purified MWCNTs showed better performance. The flexible copolymer separator not only enhanced flexibility but also served as a source of electrolyte storage. Optimization of the formulation showed active material utilization as high as 92%.

The increasing interest in portable and flexible electronics requires the development of flexible energy storage devices that can be implemented in products such as smart cards, intelligent clothing, novelty packaging as well as flexible displays and transdermal delivery patches.[1–6] Hence efforts are underway to make different flexible power sources including primary batteries, rechargeable batteries, and supercapacitors.[1,2,5–8] There is much research activity in adopting conventional batteries such as zinc-carbon and lithium ion, but at the same time new materials such as those based on nanoparticle complexes are being developed for battery and supercapacitor electrodes.[2,5,7–11] Commercially available printing methods such as dispensing[12,13] and stencil printing[14] are also being used to deposit electrode materials.

Advantages of primary batteries with aqueous electrolytes over lithium ion batteries include their eco-friendliness and ease of fabrication. The primary alkaline battery is more durable than conventional zinc-carbon under heavy load, but there have been relatively fewer reports on flexible alkaline cells.[6] An alkaline battery uses MnO_2 as the active material along with zinc anode. The electrodes are soaked in KOH electrolyte with a separator often made from a fibrous material such as cellulose or synthetic fibers. A flexible alkaline cell offers several challenges such as electrode flexibility, low internal resistance, gassing inhibition, and the retention of the electrolyte in the flexible cells.

Z. Wang, Z. Wu, Dr. N. Bramnik, Prof. S. Mitra
Department of Chemistry and Environmental Science
New Jersey Institute of Technology
161 Warren Street, Newark, NJ, 07102, USA
E-mail: somenath.mitra@njit.edu

DOI: 10.1002/adma.201304020

Of particular interest have been carbon nanomaterials such as graphene and carbon nanotubes (CNTs). Moreover, carbon textiles and carbon nanofibres with high flexibility have been used as substrates for electrode materials.[15,16] With exceptional structural, mechanical, and electrical properties, CNTs have shown many unique characteristics including high conductivity, large surface areas, excellent mechanical properties, and favorable kinetics, thus making themselves promising materials for flexible batteries. CNTs have been used in electrode materials as the conductive additive in flexible thin film batteries,[2,5] or have been made into films to serve as lightweight flexible current collectors.[17] However, most of the research has been based on more expensive singlewalled carbon nanotubes (SWCNT), and recently, composite electrodes based on multiwalled carbon nanotubes (MWCNT) have been reported.[5,18] Besides CNTs, the form of nanoadditives such as MnO_2 can also play a role in composite electrode performance.[19]

The separator in a flexible alkaline cell is a key component that needs to be strong and stable enough to endure the high pH environment while maintaining its flexibility. Although they take up more space, a polymer gel electrolyte/separator using nylon mesh as scaffold has been reported.[6] Free-standing films are preferred both as electrodes and separator so that more space can be reserved for the active material and the electrolyte. Polymer films with high ionic conductivity and flexibility are promising for battery fabrications. Both polyvinyl alcohol (PVA) and poly (acrylic acid) (PAA) have been reported as part of either polymer electrolyte or separator in flexible batteries.[1,6] PVA is known to be stable in alkaline environment, and a PVA-KOH-water system has been reported to remain stable for a period of two years.[20] The addition of PAA further increased the ionic conductivity.[21] Another advantage of these polymers is that they can also hold the electrolyte while maintaining flexibility. While the synthesis of PVA-PAA copolymers have been reported,[21–23] they are yet to be used as separator for flexible batteries.

The objective of the research published in this paper was to develop a high-performance, flexible alkaline battery with an MWCNT electrode that shows high active material utilization. Another objective was to develop copolymer separators to maintain the flexibility.

The battery structure, bendable electrodes, separator and photograph of a final cell are shown in **Figure 1**. SEM images of the electrodes are shown in **Figure 2**. All formed good cathode composites with the desired flexibility. Nanotubes could be uniformly dispersed in the active cathode material, where the functionalized CNTs showed slightly higher dispersibility. In the anode the CNTs dispersed well in presence of zinc

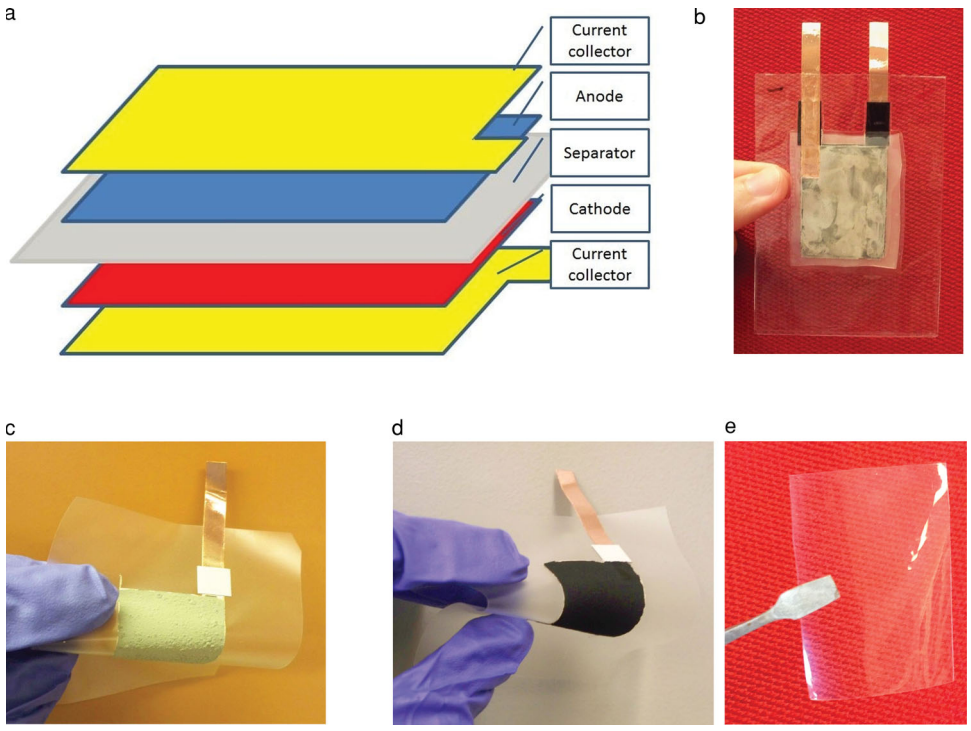

Figure 1. Fabrication of flexible battery: (a) structure of a flexible cell; (b) assembled cell; (c) anode; (d) cathode; (e) PVA-PAA copolymer separator.

particles and bridged the conductive zinc particles. The EDX data is presented in **Table 1**. It showed that other elements such as Fe existed in original CNTs as impurities, which were removed during purification. Acid functionalization introduced more oxygen into the CNTs in the form of COOH groups. The purification in dilute acids was not harsh and did not generate noticeable defects or led to oxidation.

The Fourier transform infrared (FTIR) spectra of the copolymer separator are shown in **Figure 3**. The peaks between 1700 and 1750 cm^{-1} were attributed to carbonyl C=O bonds, while the peaks between 1300 and 1000 cm^{-1} represent the C–O single bonds. The C=O peaks in the PVA spectrum can be attributed to residual acetyl in PVA, which is in line with manufacturer's analysis (http://www.sigmaaldrich.com/catalog/product/aldrich/81365). Shifts in certain peaks were observed after the esterification reaction. The acid carbonyl peak at 1717.50 cm^{-1} shifted to a higher wavenumber of 1731.96 cm^{-1}. The reaction shifted the C–O stretch and led to the appearance of two bands at 1257.70 and 1096.66 cm^{-1}. The esterification also weakened the alcohol C–O single bond absorption between 1050 and 1150 cm^{-1}.

Effects of Carbon Additives on the Cathode: Since MnO_2 has low conductivity, conductive additives were added into cathode to reduce the internal resistance of the cell. Different carbon forms were tested and the performance of the batteries were compared. The electrode resistance data for different additives are shown in **Table 2**. The application of raw CNTs instead of graphite brought the resistance down from 30.5 to 0.54 KΩ. **Figure 4** shows the discharge performance of the cells. This decrease in the cathode resistance was attributed to the fact that the CNTs created a more effective conductive network compared to graphite, leading to better performance. These results demonstrate the advantages of CNTs for electrode applications.[24] Moreover, it has been reported that alkaline metal cations interact with the phenyl group of the CNTs, resulting in cation-π interaction.[25,26]

Even though the electrode resistance was higher, the purified CNTs showed improvements over the raw CNTs (Figure 4 and **Table 3**). This was due to the removal of the metallic and nontubular carbon impurities. The metals influence the electrochemistry while the graphitic nanoparticles along with amorphous carbon are not as electrically conductive and do not form uniform composites. The acid treatment generated carboxylic groups on the surface,[27] making it more hydrophilic. Although there have been reports that the surface oxidation treatment may enhance the electronic conductivity of CNT composites,[28–30] in our experiment the functionalized CNTs were not as effective as its non-functionalized analogues. Although the functionalized CNTs showed better dispersion, the oxidative treatment created defects on the CNT surface, which disrupted charge transport (Figure 2b,c), thus compromising the overall performance. Graphite showed the poorest dispersibility (Figure 2a).

The Effect of CNT Concentrations: Increasing the CNT concentration resulted in a higher operation voltage and higher discharge capacity. However, for the same electrode weight, the amount of active material decreased as the concentration CNT increased, which reduced the overall capacity of the cell (**Figure 5**a). At higher CNT loading, the electrode materials became more fragile, which compromised the flexibility. Electrodes with more than 10% CNTs disintegrated easily. The hollow structure of the CNTs allowed it to hold the electrolyte and enhance the discharge performance; at the same time the

Adv. Mater. **2013**,
DOI: 10.1002/adma.201304020

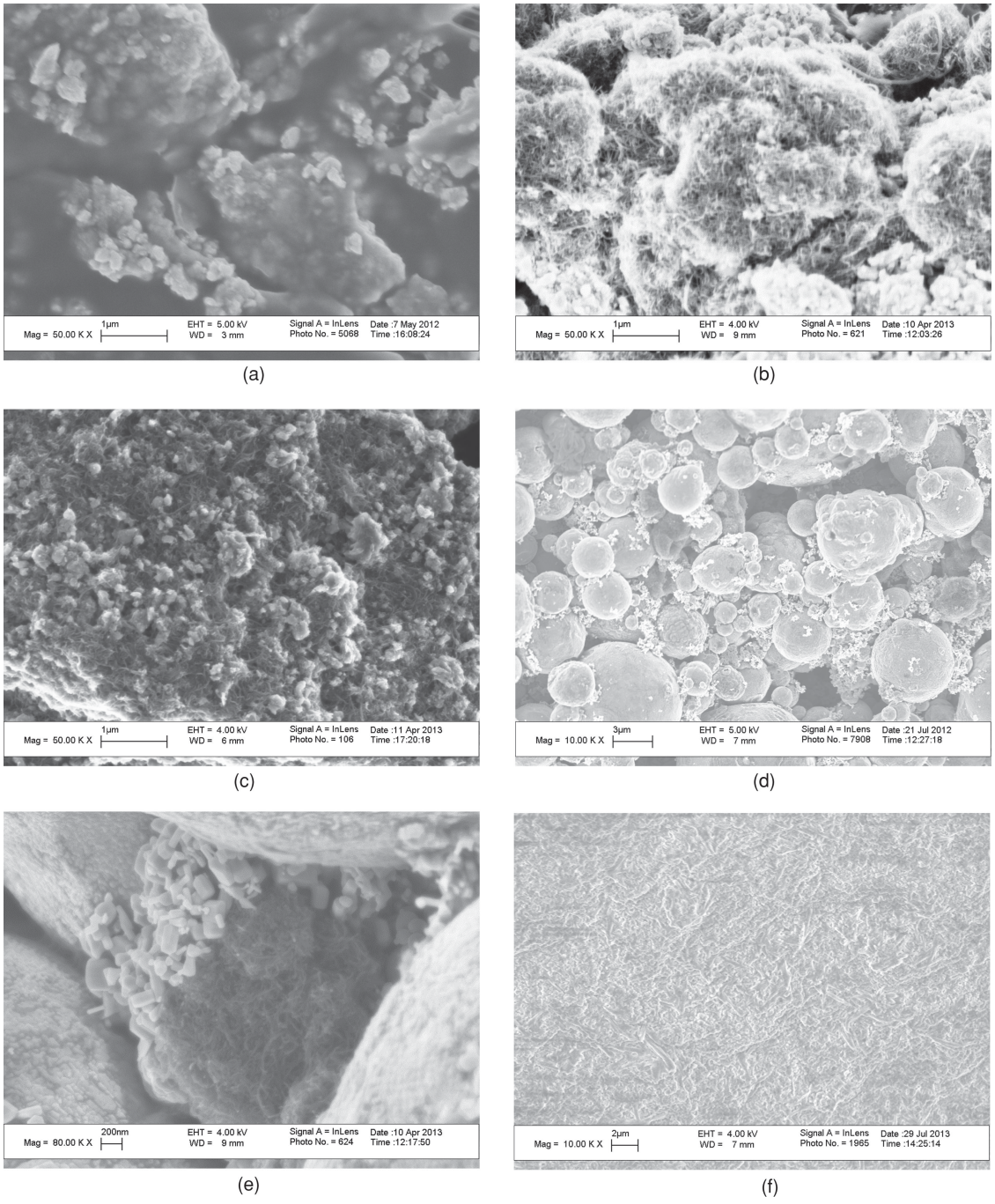

Figure 2. SEM images of electrode materials: (a) cathode with graphite; (b) cathode with purified CNTs; (c) cathode with CNT-COOH; (d) anode with micrometer-size zinc particles; (e) CNTs among zinc particles in anode; (f) copolymer separator soaked in electrolyte.

electrodes swelled as they soaked up water, and shrank as they dried out. This led to electrode cracking when there was insufficient binder to hold it together (Figure 5b). That could explain why the performance of electrodes with 15% CNTs was not as good as those at lower concentrations. To avoid this and maintain electrode flexibility, more binder was required and this decreased the conductivity and chemical reactivity. Similar was the situation with the anode.

Table 1. EDX results for CNTs.

Element weight%	Raw CNTs	Purified CNTs	Functionalized CNTs
C	94.55	94.94	92.02
O	1.36	2.59	6.85
Ni	3.74	2.47	1.13
Fe	0.34	0	0

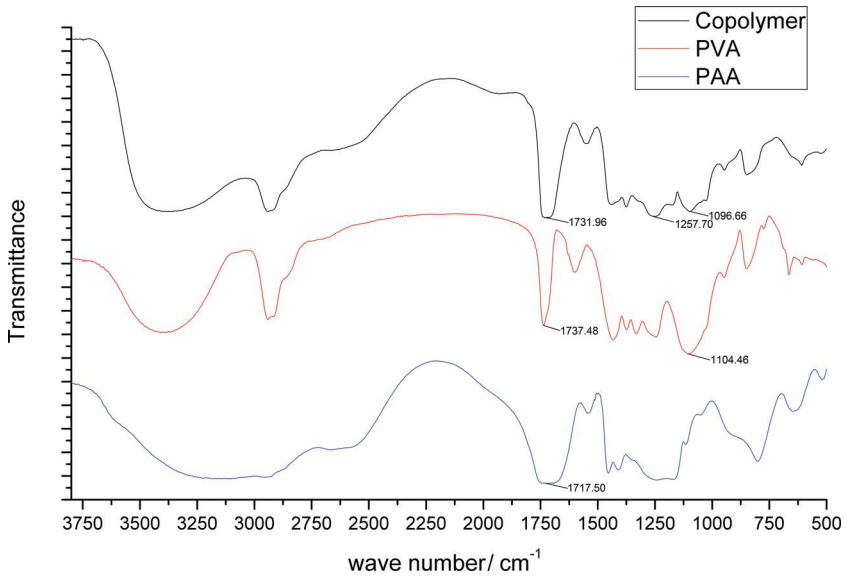

Figure 3. FTIR spectrum for PVA, PAA and the copolymer separator.

Anode Optimization: Zinc was consumed as the battery discharged, and zinc oxide was formed, which increased the internal resistance. Therefore, excess zinc was applied to the anode to maintain the electrode conductivity. Gas evolution in alkaline batteries is known to be a problem, excess ZnO has been reported to hinder zinc corrosion, and a decrease in KOH concentration is known to decrease hydrogen generation.[31] Anodic corrosion can be inhibited by the addition of certain organic compounds or metals such as Bi, Pb, and Al.[32–34] The organic and metal oxides inhibitors are nonconductive and together with polyethylene oxide (PEO) and the zinc oxide generated during the reaction, they increase the anode resistance. In order to lower the resistance, small amount of CNTs were added into the anode (**Figure 6**). In most cases, higher binder concentration led to higher flexibility but lower conductivity and performance.

Table 2. Electrode resistance of cathode materials with different conductive additives.

Conductive additive	Graphite [kΩ]	Functionalized CNTs [kΩ]	Purified CNTs [kΩ]	Raw CNTs [kΩ]
Resistance	30.5	5.4	1.9	0.54

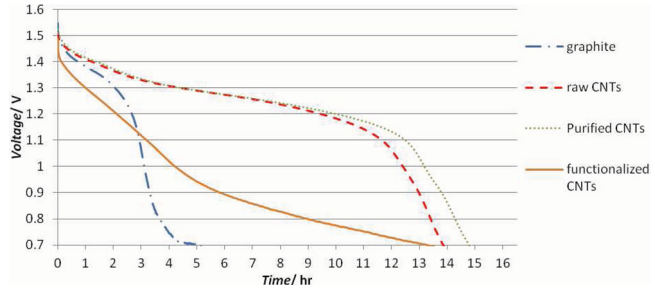

Figure 4. Discharge curves of cells with different conductive additives (in fixed cells, 2640 Ω discharge).

In other cases when there was insufficient binder, the electrode was susceptible to cracking as shown in Figure 5b, which invariably led to a decrease in the discharge performance. That was the reason why the discharge performance increased when the PEO ratio increased (Figure 6). Effects of binder concentration are also shown in Figure 5, where 6% w/w graphite was used in the cathode. Finally the formulation with 4% PEO and 2% CNTs showed optimum performance and flexibility.

Optimizing the particle size of zinc was important for controlling gas generation. Smaller, micrometer-size particles (Figure 2d) with larger surface area facilitated discharge and promoted flexibility. However, zinc nanoparticles enhanced gassing significantly and batteries ceased to work soon.

Separator Optimization: The discharge curves in **Figure 7** show that PVA-PAA copolymer film had similar performance to glass fiber separator. However the mechanical strength of the PVA-PAA was higher and it had flexibility compared to glass fiber or filter paper separator, and remained stable in the basic environment. Thicker separator held more electrolyte but compromised thickness and flexibility. According to our experimental results, 1 g of the dry PVP-PAA separator could absorb and hold approximately 2.3 g of electrolyte. An SEM image of such a separator is shown in Figure 2f. The separator also remained stable in the electrolyte. In one experiment the separator, which was soaked in the electrolyte for one month, showed no sign of decomposition.

Performance of Flexible Batteries: A constant resistance discharge pattern of a flexible battery through a 2640 Ω is shown in **Figure 8**. With an optimized formulation and copolymer separator, a 3 cm × 4 cm, 3.3 g flexible battery lasted as long as 155 hours (Figure 8). The capacity of a flexible battery obtained for optimized anode and cathode with 8% purified CNTs (283 mAh g^{-1}) corresponded to the utilization of 92% of the theoretical capacity of MnO_2 (308 mAh g^{-1}) under a 3.6mA constant current discharge with a cut off voltage 0.9 V (**Figure 9**). This was higher than what has been reported before for either

Table 3. Table specific data of cells with different cathode formulations.

Description of the Cell	Specific Energy [mWh g^{-1} cathode]	Specific Capacity [mAh g^{-1} cathode]	Specific Capacity [mAh g^{-1} MnO_2]	MnO_2 utilization [%]
6% Graphite	71.3	54.3	64.7	21.0
6% MWCNTs-raw	259	205	244	79.2
6% MWCNTs-COOH	96.0	83.7	99.6	32.3
6% MWCNTs-purified	275	218	259	84.1
3% MWCNTs-purified	213	178	205	66.6
8% MWCNTs-purified	289	230	281	91.2
10% MWCNTs-purified	297	236	295	95.6
15% MWCNTs-purified	261	211	281	91.2

Adv. Mater. **2013**,
DOI: 10.1002/adma.201304020

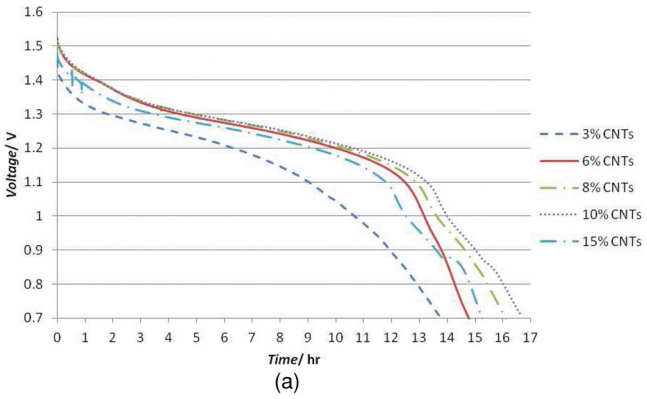

(a)

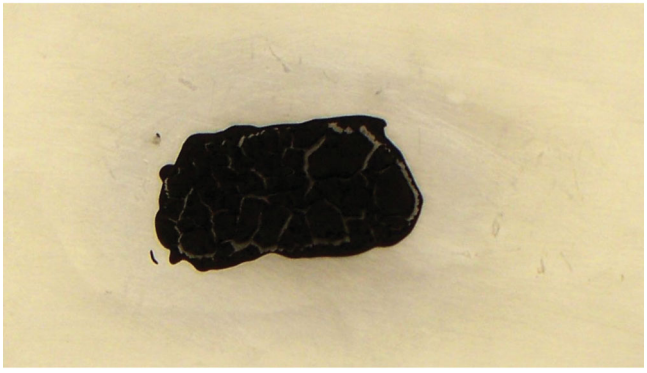

(b)

Figure 5. (a) Batteries with different amount of purified CNTs in cathodes (in fixed cells, 2640 Ω discharge); (b) cathode cracking at high CNT percent.

alkaline or zinc-carbon battery.[5,6] Discharge performances at different discharge rates are shown in Figure 8.

Discharge tests under bending conditions (3.6 mA) revealed that the batteries remained functional (**Figure 10**). Two batteries that are connected in series can light up an LED light, as shown in **Figure 11**. The overall flexibility of the battery depends on the mechanical properties of each component: electrodes, electrolyte, separator, and substrate/ packaging. The electrodes, substrate and separator showed

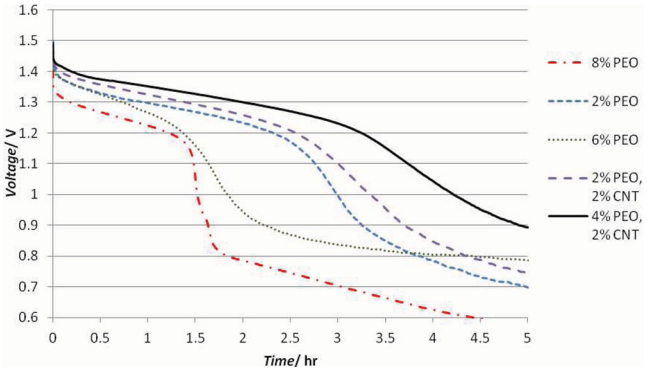

Figure 6. Effects of PEO binder and CNTs in anode, graphite in cathode (in fixed cells, 2640 Ω discharge).

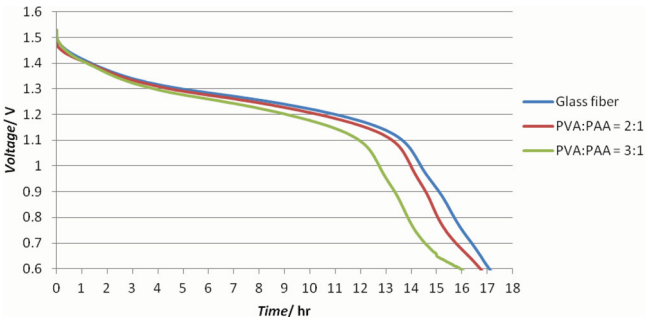

Figure 7. Cells with polymer separator/ glass fiber separator and optimized electrodes.

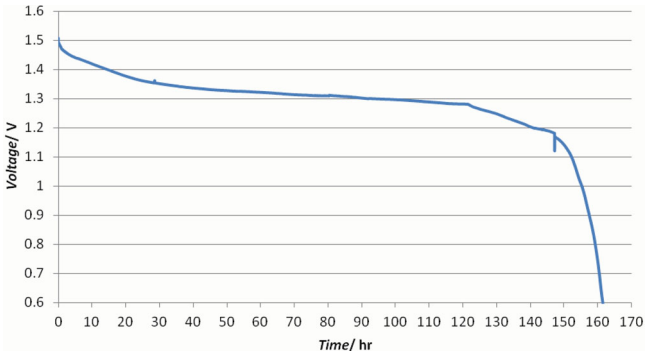

Figure 8. A flexible battery discharged under 2640 Ω constant resistance discharge.

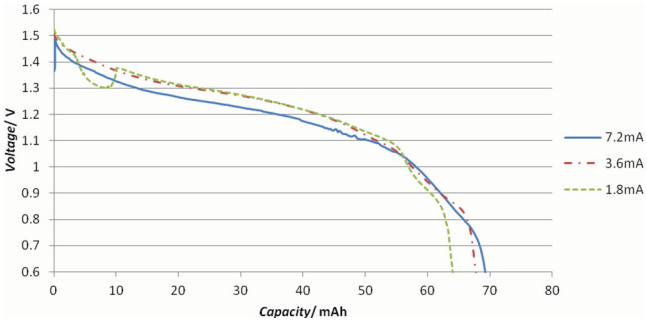

Figure 9. Discharge curves under different currents.

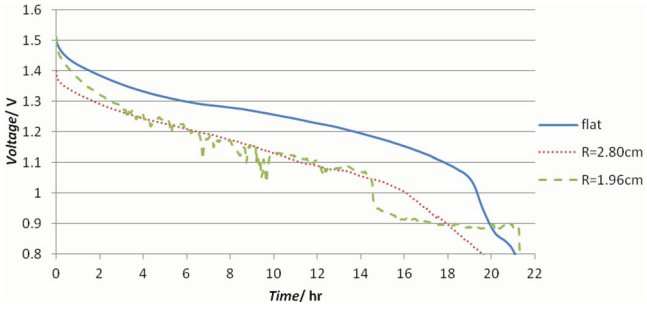

Figure 10. Discharge pattern under bending conditions.

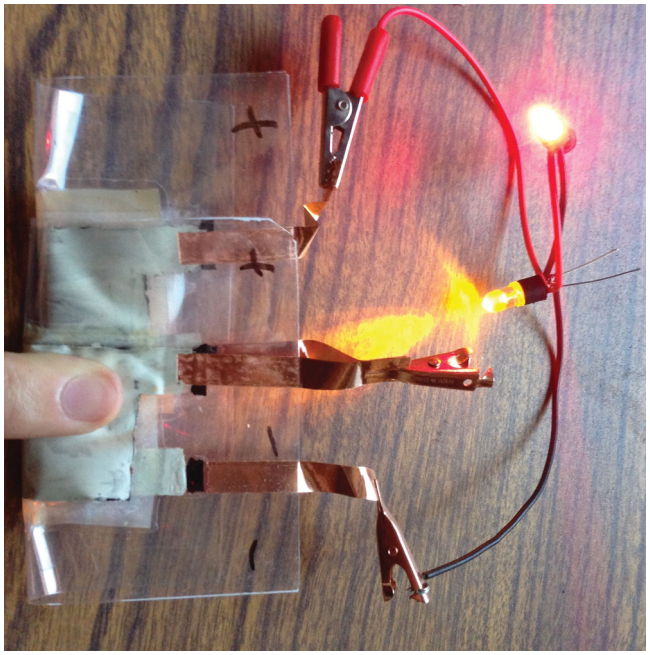

Figure 11. LED demos with flexible alkaline batteries.

acceptable flexibility (Figure 1). Bending could induce a compression of the cell stacking enhancing the contact between the particles and between the electrodes and the separator. However, it may also cause cracking in the electrode materials due to the stress. The bending test showed that batteries remained functional, though some voltage fluctuations were observed. PEO, though water-soluble, did not dissolve in high salt concentrations or in basic solutions,[35] rendering it an effective binder in flexible batteries. In one of our tests, a free-standing PEO film also remained stable in KOH solution. It is the opinion of the authors that the bending performance can be further improved by further optimization of the electrolyte/ separator and by the utilization of a more effective sealing system.

A new flexible alkaline battery with CNTs in electrode formulation and a novel separator is reported. The CNTs showed some excellent performance and utilization of MnO_2 reached as high as 92%. The PVA-PAA copolymer not only was an effective separator but also served as a means of electrolyte storage, ensuring the flexibility of the battery without performance compromise. The formulation of the alkaline battery was such that it could be printed using conventional techniques such as screen printing, stensil printing, and ink dispensing.

Experimental Section

The cathode paste was prepared by mixing electrolytic manganese dioxide powder (EMD, TRONOX, ≥ 92%, AB Grade), polyethylene oxide (PEO, Sigma Aldrich, M_v ~ 400 000) and conductive additives. Multiwalled carbon nanotubes (MWCNTs, purity 95%, diameter 20–30 nm, length 10–30 µm, Cheap Tubes Inc. Brattleboro, VT, USA) were used as received, purified or functionalized prior to the electrode preparation. Synthetic graphite (Sigma Aldrich, <20 µm) was used without further treatment. The purification and functionalization of CNTs was performed in a microwave-accelerated reaction system (Mode: CEM Mars) using a method previously published by our laboratory.[36,37]

The powders were mixed and then added into DI water, which served as the solvent. The slurry was mixed for at least 30 min, followed by 30 min of sonication using OMNI SONIC RUPTOR 250 ultrasonic homogenizer. Then, the cathode slurry was stirred again for 20 hours to form a homogeneous cathode material. The dry cathode formulation in a flexible alkaline battery contained a conductive additive (3–15%, w/w) and PEO binder (10%, w/w), with the rest being EMD. Cathode optimization was carried out with an anode that contained zinc (96%, w/w), ZnO (2%, w/w) and PEO (2%, w/w). The anode paste was prepared by mixing zinc powder (Sigma Aldrich, ≤10 µm, ≥98%), PEO as binder, zinc oxide powder (Sigma Aldrich, ≥99%) and Bismuth (III) oxide (Sigma Aldrich, 90–210 nm particle size, ≥99.8%) inhibitors, and conductive additive. The powders were mixed in the presence of DI water, and then stirred to form a homogeneous anode paste. The anode dry formulation in a flexible alkaline battery contains ZnO (2%, w/w), a conductive additive (0–2%, w/w), Bi_2O_3 (0–3%, w/w), PEO (2–8%, w/w), and the rest was zinc powder. In cases of anode optimization, cathode formulation was fixed as EMD (84%, w/w), graphite (6%, w/w), and PEO binder (10%, w/w). Scanning electron microscope (SEM) images were collected on the LEO 1530 VP Scanning Electron Microscope (Figure 2). Electrode materials were cast onto the flat surface and dried to form a 0.2 mm thick layer with a 1 cm × 1 cm area. The resistance between two ends of the layer was measured using a Keithley digital multimeter.

A copolymer film made from polyvinyl alcohol (PVA, Mowiol 18–88, Sigma Aldrich, Mv ~ 130000) and poly (acrylic acid) (PAA, Sigma Aldrich, Mv ~ 450000) was used as the separator in the flexible battery. PAA was first dissolved in 0.26% KOH solution, with mass ratio 1: 30,[22] and stirred under 80 °C till all the solids dissolved. After a sonication for 30min, extra DI water was added along with PVA. The typical PVA:PAA mass ratio here was 2:1 to get a good balance between ionic conductivity and mechanical strength.[21] The solution was stirred at 70 °C till all the PVA dissolved. After another 30 min of sonication, the solution was again stirred for another 12 hours and allowed to settle for an additional 12 hours to remove air bubbles. The fluid was then cast onto a flat smooth surface and dried. After drying, the copolymer film was peeled from the surface and heated at 150–160 °C for 50 min for crosslinking by ester linkage.[22] Typical thickness of such a copolymer film was 0.2 mm. The Fourier transform infrared spectroscopy (FTIR) of the separator film was done on a Perkin-Elmer instrument (Waltham, MA).

After applying the electrode slurry onto the current collectors, the electrodes were allowed to dry at ~60 °C for 30 minutes with the least 5 minutes under vacuum (9.893 kPa) to completely remove any residual water. For flexible cells the typical weights of the cathode and anode after drying were 0.315 and 0.64 g respectively. The electrodes were assembled facing each other with the separator between them. Before assembling, the separator was soaked in electrolyte solution, which was KOH solution (9M) with ZnO (6%). The battery was thermally sealed in a laminator.

The electrochemical performances of different formulations were measured in fixed Swagelok-type cells. In this case the electrode paste was cast directly onto the current collectors and dried. The typical weight of the cathode paste after drying was 0.03 g. For both fixed and flexible cells, the Zn anode was taken in excess in respect to MnO_2 cathode to maintain anode conductivity. Glass microfiber filters (Grade GF/A: 1.6 µm, Whatman) were used as separator in fixed Swagelok-type cells.

The flexible electrodes were prepared by casting the slurries onto the current collector made of silver ink (CAIG Laboratories Inc.) pasted directly onto the substrate. Batteries were fabricated in fixed metal cells while graphite rods (12.5 mm diameter) were used as current collectors. The flexible batteries were fabricated and encapsulated in polyethylene terephthalate (PET) film, which is coated with ethylene vinyl acetate copolymer (EVA) resin. The typical electrode area of a flexible battery was 3 cm × 4 cm. Copper foil strips stuck to the current collector served as electrode tabs. The bendable electrodes are shown in Figure 1.

The electrochemical performance of the battery was measured using MTI Battery Analyzer (Richmond, CA). They were discharged at

Adv. Mater. **2013**,
DOI: 10.1002/adma.201304020

constant resistance mode (2640 Ω) and also under constant current modes (1.8, 3.6, and 7.2 mA, respectively). For the measurement of the electrochemical performance under bending, the batteries were firmly attached over a cylindrical solid substrate of predetermined curvature.

Acknowledgements

This work was partially funded by the National Institute of Environmental Health Sciences (NIEHS) under Grant Number RC2 ES018810. Any opinions, findings, and conclusions or recommendations expressed in this material are those of the author(s) and do not necessarily reflect the views of the NIEHS.

Received: August 9, 2013
Revised: September 5, 2013
Published online:

[1] J. C. Bailey, A. Hilmi, M. A. Schubert, J. Zhang, G. Zheng, *US Patent Application 20100209756 A1* **2010**.
[2] P. Hiralal, S. Imaizumi, H. E. Unalan, H. Matsumoto, M. Minagawa, M. Rouvala, A. Tanioka, G. A. J. Amaratunga, *ACS Nano* **2010**, *4*, 2730–2734.
[3] J. A. Rogers, Z. Bao, K. Baldwin, A. Dodabalapur, B. Crone, V. R. Raju, V. Kuck, H. Katz, K. Amundson, J. Ewing, P. Drzaic, *Proc. Natl. Acad. Sci. USA* **2001**, *98*, 4835–4840.
[4] M. Rasouli, L. S. J. Phee, *Expert Rev. Med. Devices* **2010**, *7*, 693–709.
[5] Z. Wang, N. Bramnik, S. Roy, G. D. Benedetto, J. L. Zunino III, S. Mitra, *J. Power Sources* **2013**, *237*, 210–214.
[6] A. M. Gaikwad, G. L. Whiting, D. A. Steingart, A. C. Arias, *Adv. Mat.* **2011**, *23*, 3251–3255.
[7] X. Jia, C. Yan, Z. Chen, R. Wang, Q. Zhang, L. Guo, F. Wei, Y. Lu, *Chem. Commun.*, **2011**, *47*, 9669–9671.
[8] L. Hu, H. Wu, F. L. Mantia, Y. Yang, Y. Cui, *ACS Nano* **2010**, *4*, 5843–5848.
[9] Y. C. Chen, Y. K. Hsu, Y. G. Lin, Y. K. Lin, Y. Y. Horng, L. C. Chen, K. H. Chen, *Electrochim. Acta* **2011**, *56*, 7124–7130.
[10] R. K. Sharma, L. Zhai, *Electrochim. Acta* **2009**, *54*, 7148–7155.
[11] Y. Sun, S. Jiang, W. Bi, C. Wu, Y. Xie, *J. Power Sources* **2011**, *196*, 8644–8650.
[12] C. C. Ho, J. W. Evans, P. K. Wright, *J. Micromech. Microeng* **2010**, *20*, 104009.
[13] A. M. Gaikwad, J. W. Gallaway, D. Desai, D. A. Steingart, *J. Electrochem. Soc.* **2011**, *158*(2), A154.
[14] A. M. Gaikwad, D. A. Steingart, T. N. Ng, D. E. Schwartz, *Appl. Phys. Lett.* **2013**, *102*, 233302.
[15] L. Bao, J. Zang, X. Li, *Nano Lett.* **2011**, *11*, 1215–1220.
[16] L. Bao, X. Li, *Adv. Mater.* **2012**, *24*, 3246–3252.
[17] A. Kiebele, G. Gruner, *Appl. Phys. Lett.* **2007**, *91*, 144104.
[18] Y. Zhang, T. Chen, J. Wang, G. Min, L. Pan, Z. Song, Z. Sun, W. Zhou, J. Zhang, *Appl. Surf. Sci.* **2012**, *258*, 4729–4732.
[19] J. Zang, X. Li, *J. Mater. Chem.* **2011**, *21*, 10965–10969.
[20] A. A. Mohamad, N. S. Mohamed, M. Z. A. Yahya, R. Othman, S. Ramesh, Y. Alias, A. K. Arof, *Solid State Ion.* **2003**, *156*, 171–177.
[21] G. M. Wu, S. J. Lin, C. C. Yang, *J. Membr. Sci.* **2006**, *275*, 127–133.
[22] K. Kumeta, I. Nagashima, S. Matsui, K. Mizoguchi, *J. Appl. Polym. Sci.* **2003**, *90*, 2420–2427.
[23] H. H. Wang, T. W. Shyr, M. S. Hu, *J. Appl. Polym. Sci.* **1999**, *74*, 3046–3052.
[24] X. Zhang, Y. Cui, Z. Lv, M. Li, S. Ma, Z. Cui, Q. Kong, *Int. J. Electrochem. Sci.* **2011**, *6*, 6063–6073.
[25] G. Mpourmpakis, E. Tylianakis, D. Papanikolaou, G. Froudakis, *Rev. Adv. Mater. Sci.* **2006**, *11*, 92–97.
[26] G. W. Gokel, S. L. De Wall, E. S. Meadows, *Eur. J. Org. Chem.* **2000**, *2000*, 2967–2978.
[27] F. Valentini, A. Amine, S. Orlanducci, M. L. Terranova, G. Palleschi, *Anal. Chem.* **2003**, *75*, 5413–5421.
[28] Y. Liu, L. Gao, *Carbon* **2005**, *43*, 47–52.
[29] Z. Spytalsky, C. Krontiras, S. Georga, C. Gallotis, *Composites A: Appl. Sci. Manufact.* **2009**, *40*, 778–783.
[30] Q. Li, Y. Li, X. Zhang, S. Chikkannanavar, Y. Zhao, A. Dangelewicz, L. Zheng, S. Doorn, Q. Jia, D. Peterson, P. Arendt, Y. Zhu, *Adv. Mater.* **2007**, *19*, 3358–3363.
[31] V. Ravindran, V. S. Muralidharan, *J. Power Sources* **1995**, *55*, 237–241.
[32] A. R. Suresh Kannan, S. Muralidharan, K. B. Sarangapani, V. Balaramachandran, V. Kapali, *J. Power Sources* **1995**, *57*, 93–98.
[33] J. Y. Huot, E. Boubour, *J. Power Sources* **1997**, *65*, 81–85.
[34] J. Dobryszyckia, S. Biallozor, *Corros. Sci.* **2001**, *43*, 1309–1319.
[35] M. J. Hey, D. P. Jackson, H. Yan, *Polymer* **2005**, *46*, 2567–2572.
[36] Y. Chen, Z. Iqbal, S. Mitra, *Adv. Funct. Mater.* **2007**, *17*, 3946–3951.
[37] Y. Chen, S. Mitra, *J. Nanosci. Nanotechnol.* **2008**, *8*, 5770–5775.